

A Study with the EDGE2D Code of the Power Exhaust Problem in ITER Relevant Divertor Plasmas

A Taroni, G Corrigan, R Simonini, J Spence, S Weber.

JET Joint Undertaking, Abingdon, Oxon, OX14 3EA.

"This document is intended for publication in the open literature. It is made available on the understanding that it may not be further circulated and extracts may not be published prior to publication of the original, without the consent of the Publications Officer, JET Joint Undertaking, Abingdon, Oxon, OX14 3EA, UK".

"Enquiries about Copyright and reproduction should be addressed to the Publications Officer, JET Joint Undertaking, Abingdon, Oxon, OX14 3EA".

INTRODUCTION

Power exhaust in the ITER divertor is an important problem to be solved for the design of this device. A solution based on plasma extinction was suggested by P. H. Rebut and M. L. Watkins [1].

Plasmas that practically extinguish (detached plasmas) in the divertor region have been observed in several Tokamaks, including JET. These plasmas are obviously of great interest for possible extrapolations to ITER. However such extrapolations require a better degree of understanding of the mechanisms leading to plasma detachment than it is presently available.

As a step in this direction an extensive campaign of numerical simulations based on the EDGE2D/U- NIMBUS chain of codes [2] has been carried out at JET in order to study some basic problems related to plasma detachment. In particular we studied the dependence of detachment on mid-plane separatrix density, power entering the SOL, volume power losses in the SOL and geometrical configuration.

Most of the results reported refer to predictions for the JET Mk I divertor. JET operations only started very recently and a comparison between experimental results and these predictions has not yet been possible. However the code reproduce important trends observed in detached plasmas in the old JET divertor configuration.

The modelling assumptions used can be found in refs [3] and [4]. Atomic data are from the ADAS data base[5]. It is shown in [4] that the transport model we are using allows reasonable simulations of attached L-mode plasmas.

EFFECTS RELATED TO MID-PLANE SEPARATRIX DENSITY, POWER ENTERING THE SOL AND GEOMETRY IN A PURE PLASMA

Experimental results in detached plasma regimes suggest that particle, total momentum and total energy flows are strongly reduced at the divertor targets with respect to the case of attached plasmas with comparable values of input power in the SOL and density upstream. Conservation laws imply that such a reduction must be the result of volume loss mechanisms for momentum and energy and possibly of perpendicular transport toward the side walls.

We have studied the efficiency in determining detachment of volume losses alone, by assuming in our computations a set of boundary conditions giving no flux of particles or energy towards the side walls.

In our model the volume power losses are due to both hydrogenic plasma and impurity atomic processes, while volume losses in the momentum balance are related to hydrogenic plasma atomic processes. In particular, as pointed out in [6]-[7], momentum can be efficiently dissipated via charge exchange if the plasma close to the targets enters a regime ($T \leq 5\text{eV}$ and not too high density) where the charge exchange mean free path is much shorter than the ionization mean free path, but long with respect to the width of the divertor plasma channel.

For extrapolations to ITER it is important to understand the relative role of the various loss terms in determining detachment.

We consider first the case of a pure plasma and present the results obtained for two equilibrium configurations ($I_p = 3\text{MA}$) in the Mk I divertor. (fig 1, SD case and fig 2, V case). By changing the particle inventory N in the boundary region we performed scans in the value n_s of the density at the separatrix mid-plane for two values of the SOL input power, $P = 2.5\text{MW}$ and $P = 10\text{MW}$, for each configuration (see [3] for the technique).

The main results are illustrated in figs 3 and 4 for the V configuration. Fig 3 shows how the percentage of the power P contributing to the target power load depends on

the density n_s . The values include contributions to both targets. Due to purely geometrical reasons a uniform distribution of the power entering the SOL results in somewhat more power reaching the external target, but the asymmetry is usually not too large ($\leq 50\%$). The figure also shows the contribution due to recombination at the targets, P_{rec} , which is proportional to the particle flow Φ to the targets.

The ratio f_p of the pressure at mid-plane to the pressure at the targets (related to the efficiency in dissipating parallel momentum), is shown for the same cases in fig 4. Values at the separatrix and at a field line approximately 1 cm outside are given. An average of the pressure at the targets is considered in the definition of f_p (the in-out asymmetry is small, $\leq 20\%$).

One sees that as n_s increases, the fraction of power reaching the targets decreases, while the pressure drop increases. However the power due to recombination at targets slightly increases with n_s , implying that Φ increases and that real detachment is not achieved in any of these cases. The maximum value $\Phi \approx 6.7 \cdot 10^{23} \text{ s}^{-1}$ is for $P=10\text{MW}$, $n_s \approx 4.4 \cdot 10^{19} \text{ m}^{-3}$.

The figures show that the volume loss terms in a pure plasma become more efficient at low input power, but do not seem to be enough to cause detachment if $P \geq 2.5 \text{ MW}$. The problem is mainly related to power dissipation. A similar result was obtained in [8] for both JET and ITER parameters in a slab divertor channel approximation.

Similar trends have been found for the SD configuration. However in this case the efficiency in removing momentum is somewhat less than in the V configuration. For example it results $f_p=8$ at the separatrix and $f_p=28$ at the magnetic field line 1 cm outside in a SD case with $n_s = 4.2 \cdot 10^{19} \text{ m}^{-3}$ and $P=2.5\text{MW}$. In a V case with the same value of P and somewhat lower density, $n_s = 3.7 \cdot 10^{19} \text{ m}^{-3}$, one has $f_p=40$ at the separatrix and $f_p=16$ at the magnetic field line 1 cm outside.

The reason for this is mainly related to effects of the target inclination on neutral reflection and as a consequence on the plasma profiles [3]. In the V case the divertor plasma enters more easily the low temperature regime favourable to momentum

dissipation by charge exchange. The choice of the boundary conditions towards the walls might also have an effect that remains to be assessed.

EFFECT OF IMPURITY RADIATION

A first step in studying the role of impurity radiation in plasma detachment can be performed without simulating in a consistent way impurity generation, transport and radiation. The basic feature of impurity radiation is to reduce the power flowing to the targets and it is interesting to assess how this feature in itself can modify the other flows to the targets (momentum and particles) by reducing the temperature and therefore guiding the plasma into a regime where momentum dissipation due to the hydrogenic species becomes important.

To this purpose we carried out a series of simulations using a simple formula for the radiation efficiency proposed in [9] to simulate carbon radiation in an otherwise pure ASDEX plasma.

The radiation loss term in this approximation is given by:

$$Q_{\text{rad}}(T_e) = \alpha_{\text{imp}} n^2 L_z(T_e) \quad (1)$$

$$L_z(T_e) = 2 \cdot 10^{-18} / (T_n^{1.5} + T_n^{-3}) \quad \text{erg cm}^3/\text{s} \quad (2)$$

$$T_n = \max(10^{-6}, T_e/15\text{eV}) \quad (3)$$

α_{imp} is spatially constant and in EDGE2D/U its value is determined at each time step in order to obtain a prescribed value of the total radiated power P_{RI} .

The main results obtained with this approach have been reproduced, as we will show, also by a number of simulations dealing consistently with impurities.

We found that if the conditions of a pure plasma are such that efficient radiation is expected from eqs (1)-(3), i.e. $T \leq 15\text{eV}$ at the targets, detachment can be obtained at large enough values of P_{RI} and it improves as $P - P_{\text{RI}}$ decreases. This is valid, obviously with differences related to the geometrical configuration similar to those

pointed out in the previous section, for all of the JET divertor configurations studied so far, including the pre-'92 one and a gas box configuration that are not considered here. In particular, for all the configurations tested, the value of f_p increases as $P-P_{RI}$ decreases and for this reason practically no limit related to insufficient momentum dissipation is found in the fraction of power that can be radiated.

Figs 5 and 6 illustrate the dependence of detachment on $P-P_{RI}$ in the case of the V configuration. These figures refer to an input power $P=10\text{MW}$ and a particle inventory N corresponding to a density $n_s=3.4 \cdot 10^{19} \text{ m}^{-3}$ in the case without impurity radiation.

The variation in the target power load due to recombination shown in fig.5 corresponds to a reduction of the particle flow Φ to the targets from $5.9 \cdot 10^{23} \text{ s}^{-1}$ without impurity radiation to 10^{23} s^{-1} with $P_{RI} = 8\text{MW}$.

Fig.7 shows that the density as well as the pressure drops at the targets, a clear sign of detachment. All these drops are of course related and imply a concomitant drop in neutral density.

The same figure shows that n_s slightly decreases as P_{RI} and detachment increase. This variation of n_s may depend on the transport model, the spatial distribution of impuriy radiation and the boundary conditions towards the side walls. However this is not expected to modify substantially the finding that no strong increase in n_s is required for a transition from an attached to a detached situation induced by an increase in P_{RI} . This may be related to the fact that electron heat conduction and volume energy losses still play a role at the entrance of the detachment region, and the temperature is free to drop below 5eV , contrary to the assumptions in [6].

In our simulations the role of high density n_s in detached plasmas is to reduce the temperature close to the targets and to favour the radiation losses.

Contour plots of T_e for the case $P-P_{RI} = 4\text{MW}$ are given in fig.8. The divertor region with $T \leq 5\text{eV}$ and reduced ionization appears to be large. This region becomes larger in an even more detached plasma and the divertor closure to neutrals worsens as the ionization region shifts outside the divertor.

A proper evaluation of the spatial distribution of impurity radiation in the SOL and divertor regions require a proper, consistent modelling of impurities. A few exploratory runs with the multispecies version of EDGE2D/U have been carried out in order to study this important problem. The same transport model for impurities and main plasma ions has been assumed.

Results obtained so far show that physical sputtering of Beryllium and Carbon is too low to produce enough impurities to radiate the required level of power for detachment. Injection of Carbon from the walls (that might be interpreted as a very crude simulation of chemical sputtering) can produce the level of Carbon (1-2%), required to radiate a few MWatts in the SOL.

For example in the V configuration, with 10MW input power and $N (\Rightarrow n_s = 3.4 \cdot 10^{19} \text{ m}^{-3})$ one obtains $P_{\text{RI}} = 4.5 \text{ MW}$ by assuming a carbon influx $\Phi_C \approx 10^{22} \text{ s}^{-1}$ uniformly distributed along the vacuum chamber . However in this case 70% of P_{RI} as well as 67% of Carbon is above the X-point, where Z_{eff} reaches 1.7. Results of course may differ with impurity species, and impurity injection scheme.

With eqs 1-3 only 25% of the radiation comes from above the x-point for the same P_{RI} (this fraction increases with P_{RI}), however even if the radiation patterns are different the effects of radiation on parameters relevant for detachment (f_p etc.) are similar, as expected.

Even if the most important parameters determining the accessibility to detached divertor plasma regimes appear to be $P - P_{\text{RI}}$ and n_s , the geometrical configuration might play an important role also.

For example as indicated in the previous section the SD configuration appears to be less favourable to detachment than the V configuration. Namely for the same power radiated by impurities the V configuration allows plasmas somewhat more detached, at a lower density n_s , than the SD one. In addition it is much more closed to neutrals. This is illustrated in the following table, where n_s is in 10^{19} m^{-3} , power is in MW, and $S_{\text{H,out}}$ is the percentage of ionization source distributed above the X-point.

	n_s	P	P_{RI}	P_t	P_{rec}	$F_{p,sep}$	$F_{p,1}$	SH_{out}
SD	3.8	10	4	3.25	1.23	2.9	12	7
V	3	10	4	3.5	0.7	35	3	0.9
SD	2.8	10	8	0.6	0.3	28	160	39
V	2.2	10	8	0.7	0.2	380	32	10

We remark that while the models used in EDGE2D/U are far from being properly validated against experimental observations, the trends observed in our results are very similar to those observed in detached plasmas obtained in the past in JET. This is confirmed by computations carried out with the old JET configuration and direct comparisons with the experimental information available [10], [11].

CONCLUSION

Our numerical simulations indicate that plasma extinction is unlikely in JET for relevant values of P and n_s without a means to dissipate power in the divertor (or before entering it) other than volume losses related to the atomic processes possible in a pure D or D-T plasma. A similar conclusion is likely to be true for ITER.

It appears that a solution to the power handling problem by plasma extinction in a ITER relevant divertor might imply the dissipation of power by means of impurity radiation. Clearly this requires injection of a recyclable impurity, such as neon or argon, in order to avoid impurity accumulation at targets and walls. The production of intrinsic impurities via sputtering would be minimized inside the divertor with an extinguished plasma, and it would also be small outside if the divertor remained sufficiently closed to neutrals.

Obviously a much greater understanding of impurity control and transport in the SOL than is presently available is required to assess the feasibility of such a solution. Only a careful analysis of experimental results and the validation and improvement of models on the basis of such results can help in this task.

Acknowledgments: K. Borrass, L. Horton, A. Loarte, and G. Vlasses are acknowledged for useful discussions.

REFERENCES

- [1]Watkins, M.L., Rebut, P.-H., 19th Europ. Conf. on Contr. Fusion and Plasma Phys., Innsbruck, 1992.
- [2]Simonini, R., Corrigan, G., Radford, G., Spence, J., Taroni, A., Contributions to Plasma Physics, Vol.34, 368, 1994.
- [3]Taroni, A., Corrigan, G., Simonini, R., Spence, J., Vlasses, G., Contributions to Plasma Phys., Vol.34, 448, 1994
- [4]Loarte, A.,Chankin, A., Clement, S., et al., 11th PSI Conference, Mito, Japan, (1994)..
- [5]Summers, H.,P. and von Hellermann, JET report, JET-P(93)35, 1993.
- [6]Borrass K. and Stangeby, P.,20th Europ. Conf. on Contr. Fusion and Plasma Phys., Lisbon 1993.
- [7]Stangeby. P., Nuclear Fusion, Vol. 33, 1695, 1993.
- [8]Weber, S., Simonini, R., Taroni, A., Contributions to Plasma Phys., Vol. 34, 374, 1994.
- [9]Schneider, R., Braams, B., Reiter, D., et al., Contributions to Plasma Phys., Vol. 32, 450, 1992
- [10]Taroni, A., Horton, L., Loarte, A.,et al. Workshop on ITER Divertor Physics Design, ITER JCT, Garching, Feb. 1994.
- [11]Matthews, G., F., 11th PSI Conference, Mito, Japan, (1994)..

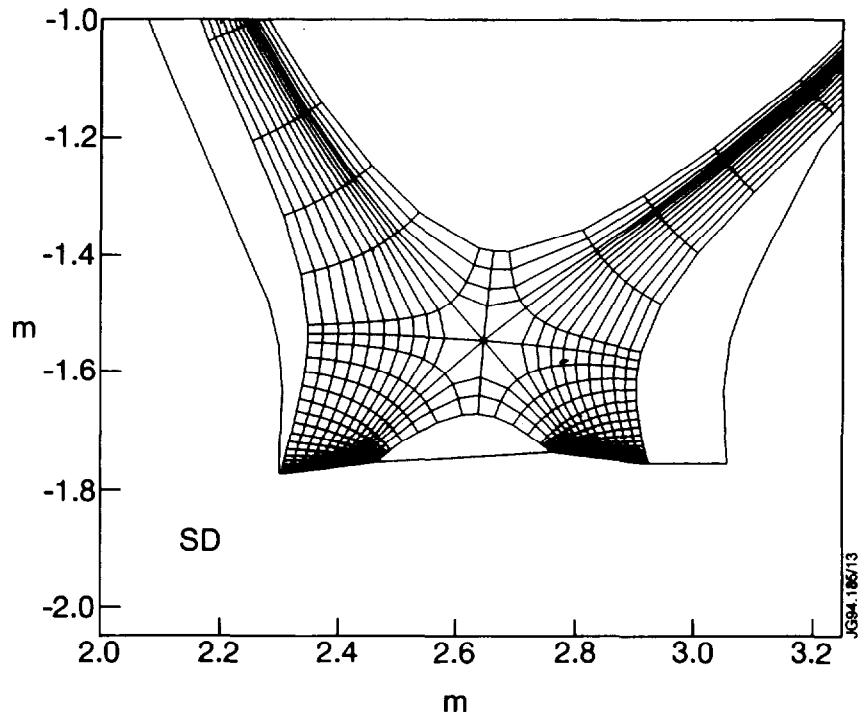


Fig1 SD configuration. Mesh from MHD equilibrium (divertor region).

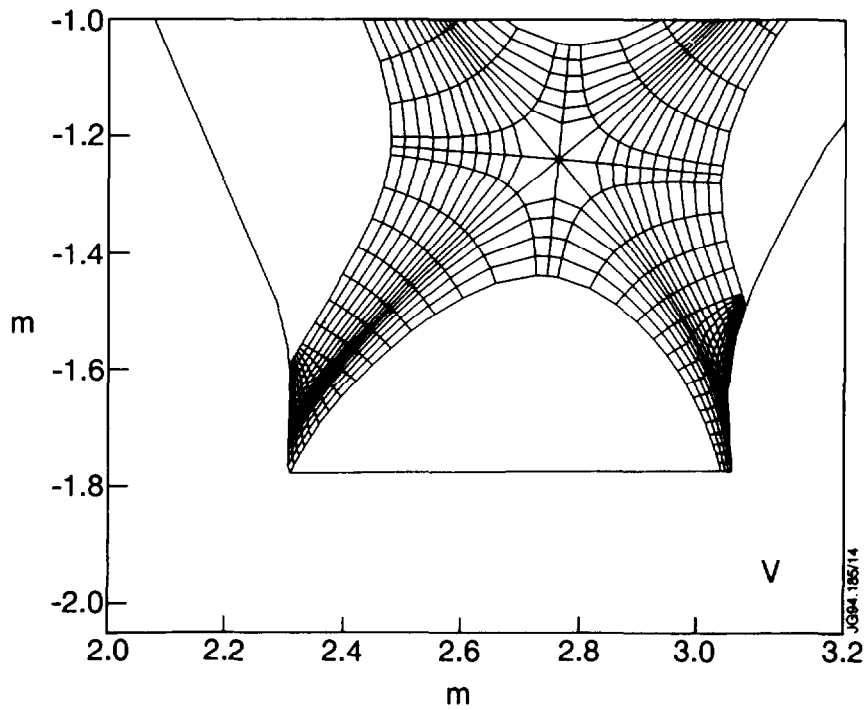


Fig2 V configuration. Mesh from MHD equilibrium (divertor region).

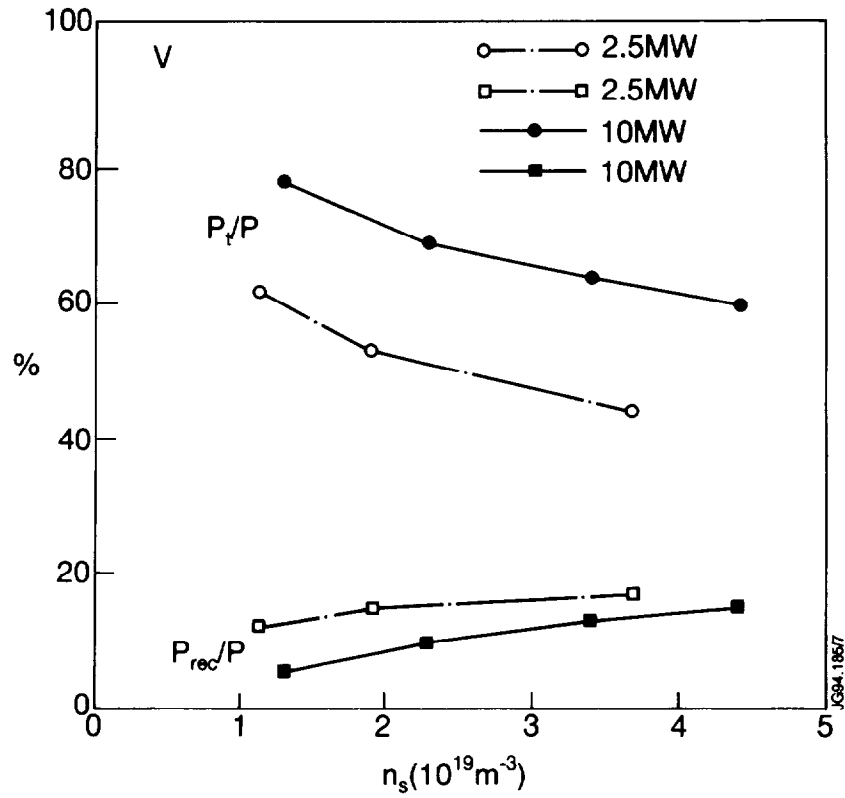


Fig3 V configuration. Percentage of input power contributing to target load and of power due to recombination at targets as a function of n_s .

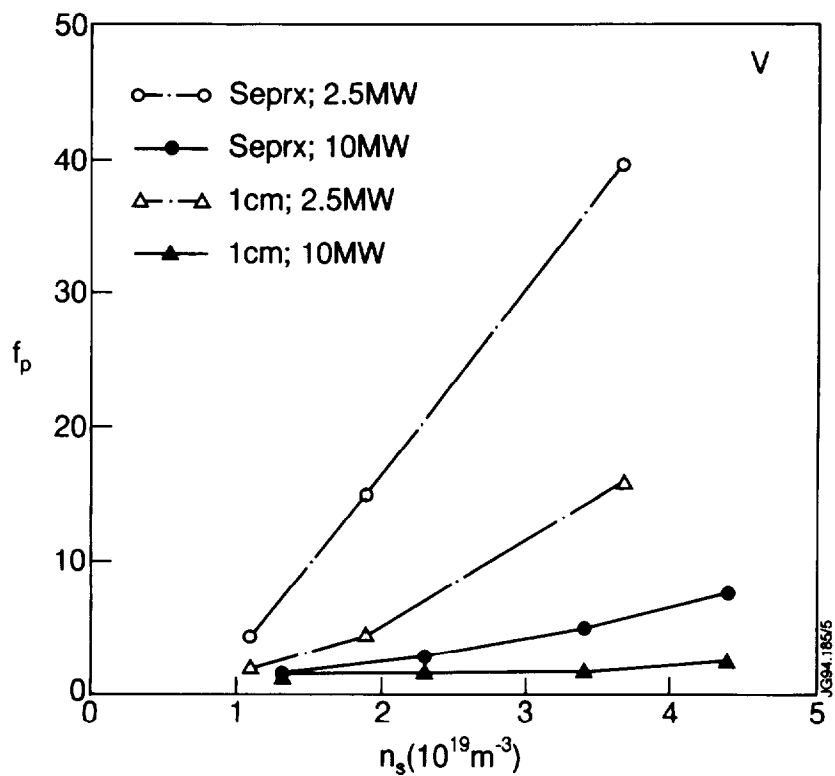


Fig4 V configuration. Pressure drop ratio f_p as a function of n_s .

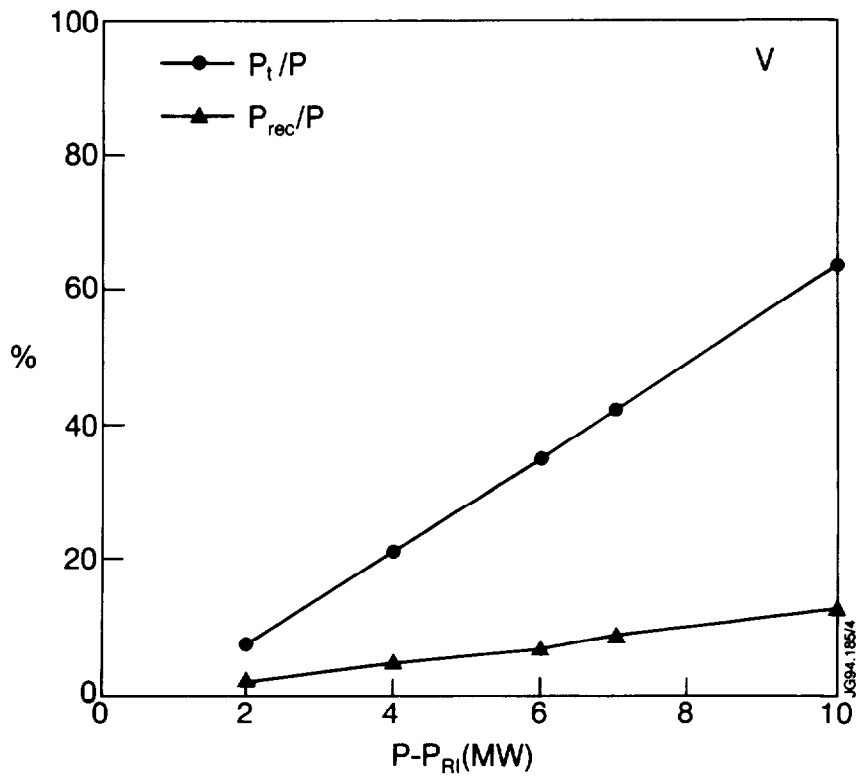


Fig 5 V configuration. Percentage of input power contributing to target load and of power due to recombination at targets as a function of $P-P_{RI}$.

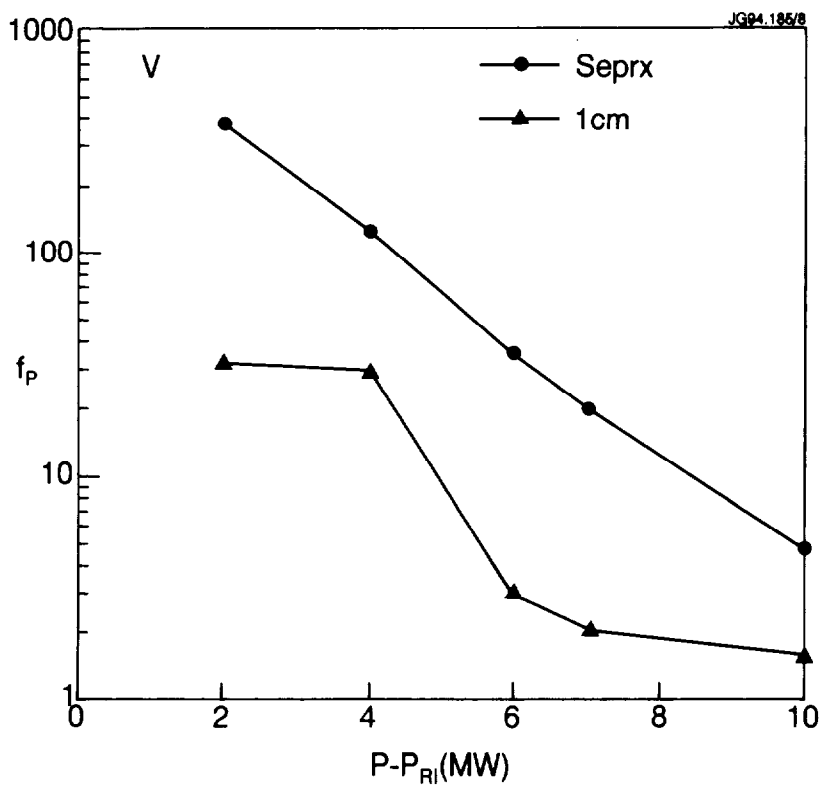


Fig6 V configuration. Pressure drop ratio f_p as a function of $P-P_{RI}$.

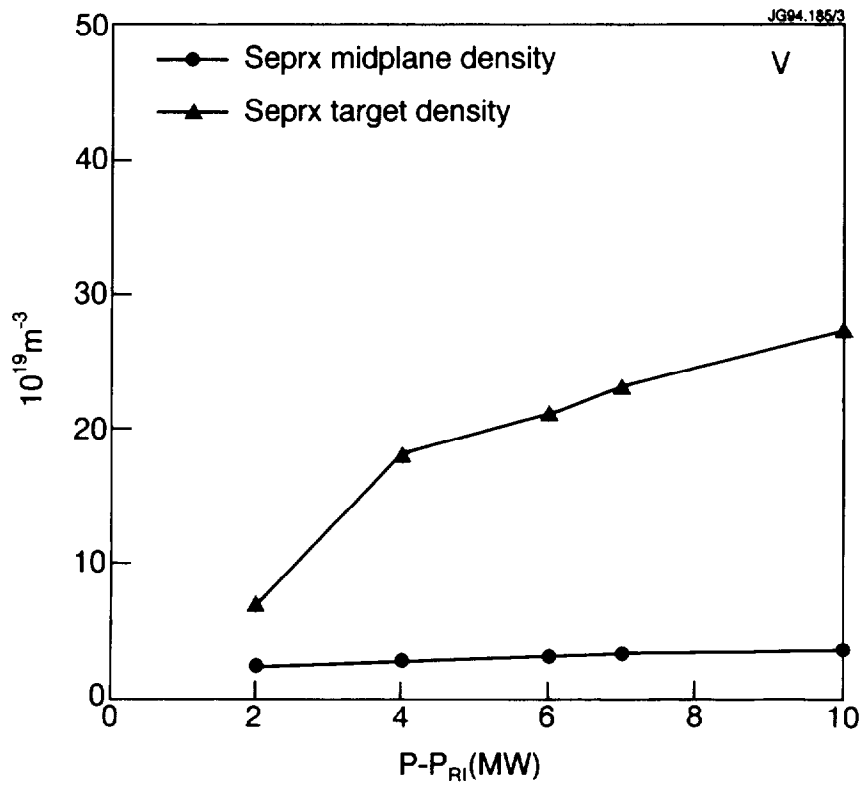


Fig 7 V configuration. Density at separatrix (mid-plane and target) as a function of P_{RI} .

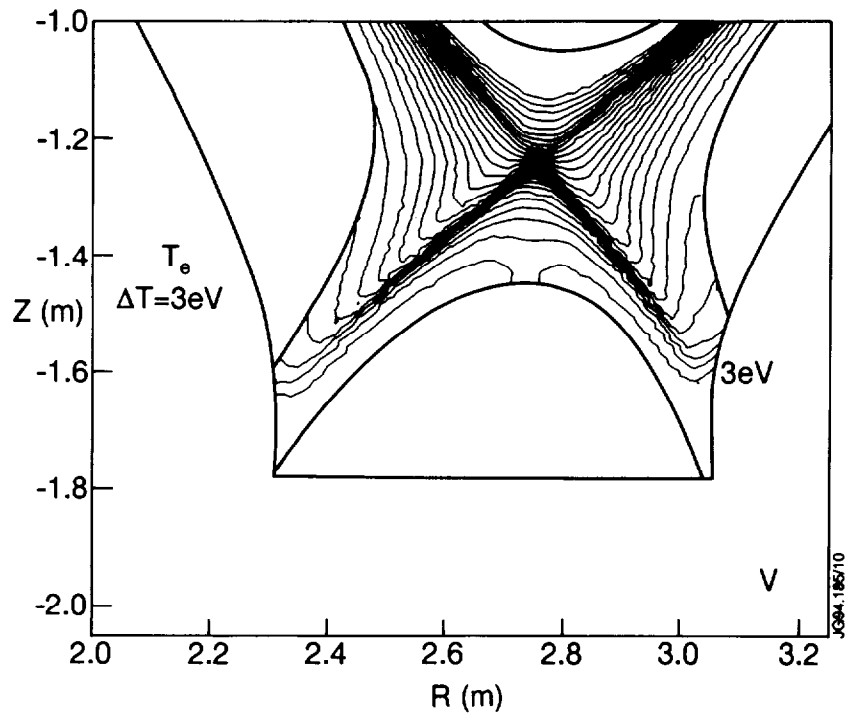


Fig 8 V configuration. Contour plot of T_e for the case $P_{RI} = 4 \text{ MW}$.